SYNTHESIS AND CHARACTERIZATION OF THIOSEMICARBAZONE LIGANDS

2.1 Introduction

Heterocyclic thiosemicarbazones and their metal complexes are of considerable interest due to their significant biological activity [1-4] and medicinal properties. Thiosemicarbazones are compounds with versatile structural features [5, 6] and they can coordinate to the metal either as a neutral ligand or as a deprotonated anion through the N, N, S or O, N, S donor atoms [7]. The two NNS donors used for the preparation of the metal complexes are:

1. 2-Benzoylpyridine *N*(4)-cyclohexylthiosemicarbazone (HL^1) {Phenyl (pyridine-2-yl) methanone *N*-cyclohexylthiosemicarbazone}

2. 2-Benzoylpyridine *N*(4)-phenylthiosemicarbazone (HL^2) {Phenyl (pyridine-2-yl) methanone *N*-phenylthiosemicarbazone}

This Chapter deals with the synthesis and spectral characterization of ligands. It also deals with X-ray diffraction studies of HL^1. The general structure and the numbering scheme of the two thiosemicarbazones are given in Fig. 2.1. This numbering scheme, according to the IUPAC system, is used throughout the entire work, except in sections 2.4.2., 2.4.5. and 2.4.6.

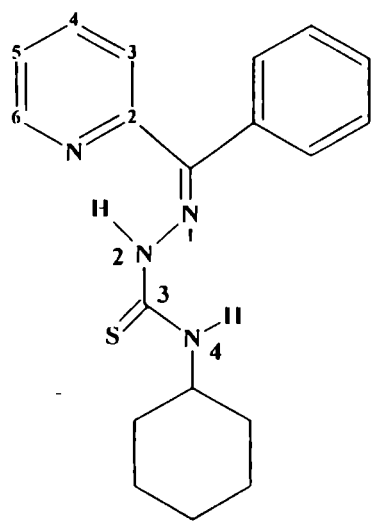

HL^1

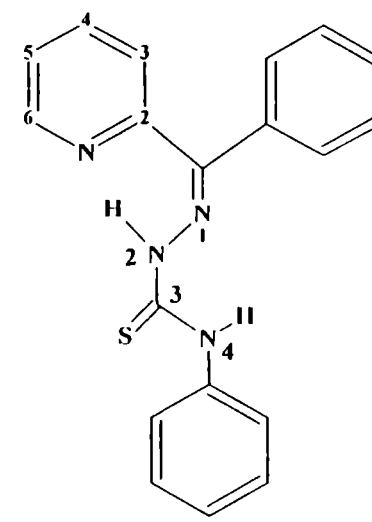

HL^2

Fig.2.1. Structural formulas of thiosemicarbazones HL^1 and HL^2

2. 2. Synthesis of thiosemicarbazones

Some general methods used for the synthesis of thiosemicarbazones are given below.

Method 1: By the condensation of a thiosemicarbazide, prepared from an aryl, aralkyl, or alkyl isothiocyanate and hydrazine, with an aldehyde or ketone.

Method 2: By the condensation of an aldehyde or ketone with methyl hydrazine carbodithioate to form an intermediate. The *S*-methyl group of the latter compound, upon displacement by an amine, forms the desired thiosemicarbazone.

Method 3: By the condensation of an isothiocyanate with the hydrazone of an aldehyde or ketone.

2.2.1. Synthesis of 2-benzoylpyridine N(4)-cyclohexylthiosemicarbazone (HL^1)

The thiosemicarbazone was prepared by adopting a reported procedure of Klayman [1].

Chemicals used

Cyclohexyl isothiocyanate (Fluka), hydrazine hydrate (Lancaster), 2-benzoylpyridine (Lancaster), methanol, acetic acid.

Method

Step 1: Cyclohexyl isothiocyanate 7.1 ml (50 mmol, 7.062 g) in 50 ml methanol and hydrazine hydrate 2.4 ml (50 mmol) in 50 ml methanol were mixed with constant stirring. The resulting solution was kept in stirred condition for 0.5 hr. The white product, *N*-cyclohexylthiosemicarbazide formed was washed with methanol and dried. m.p. 140 °C.

Step 2: *N*-Cyclohexylthiosemicarbazide (50 mmol, 8.65 g) was dissolved in 100 ml methanol. To this solution, a methanolic solution of 2-benzoylpyridine (50 mmol, 9.16 g) was added. 2 or 3 drops of acetic acid were added and refluxed for 5 hrs. The volume of the solution was reduced to half. The pale yellow crystals, separated on cooling, were filtered, washed with methanol, recrystallised from ethanol and dried over P_4O_{10} *in vacuo*. m.p.170 °C.

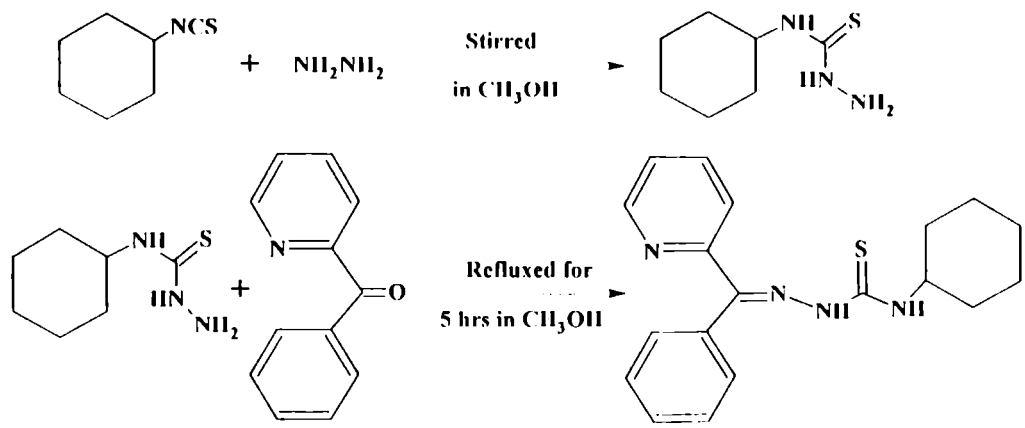

Scheme for the synthesis of HL^1

2.2.2. Synthesis of 2-benzoylpyridine N(4)-phenylthiosemicarbazone (HL^2)

Chemicals used

Phenyl isothiocyanate (Fluka), hydrazine hydrate (Lancaster), 2-benzoylpyridine (Lancaster), methanol, acetic acid.

Method

Step1: Phenyl isothiocyanate 5.9 ml (50 mmol, 6.759 g) in 50 ml methanol and hydrazine hydrate 2.4 ml (50 mmol) in 50 ml methanol were mixed with constant stirring. The resulting solution was kept in stirred condition for 0.5 hr. The white product, *N*-phenylthiosemicarbazide formed was washed with methanol, and dried. m.p. 125 °C.

Step 2: *N*-Phenyl thiosemicarbazide (50 mmol, 8.35 g) was dissolved in 100 ml methanol. To this solution, a methanolic solution of 2-benzoylpyridine (50 mmol, 9.16 g) and 2 or 3 drops of acetic acid were added and refluxed for 5 hrs. The volume of the solution was reduced to half. The dark brown crystals, separated on cooling, were washed with methanol, recrystallised from ethanol and dried over P_4O_{10} *in vacuo*. m.p.135 °C.

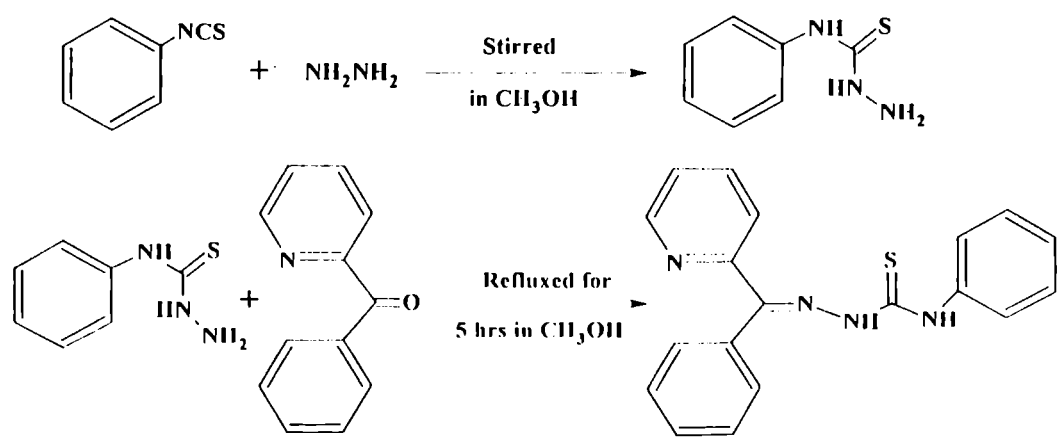

Scheme for the synthesis of HL^2

2.3. Physical measurements

Details regarding the analytical measurements and various spectral techniques are given in Chapter 1.

2.3.1. X- Ray crystallography

Slow evaporation of the ligand in methanol yielded single crystals suitable for X-ray analysis. A pale yellow crystal of HL^1 was mounted on a glass fiber with epoxy cement for the crystallographic study. The crystallographic data and structure refinement parameters for the compound at 293 K are given in Table 1. The data were collected using a SMART CCD diffractometer equipped with graphite-monochromated Mo K_α radiation, with a detector distance of 5 cm and swing angle of -35°. A hemisphere of the reciprocal space was covered by

combination of three sets of exposures. Each set had a difference of angle (0, 88°, 180°) and each exposure of 10s covered 0.3° in *ω*.

2.4. Results and discussion

2.4.1. Synthesis

The empirical formulas, melting points and partial elemental analyses of the ligands are listed in Table 2.1. The two thiosemicarbazones HL^1 and HL^2 are pale yellow and brown colored crystals respectively. Crystals of HL^1 suitable for X-ray diffraction studies were obtained by slow evaporation from methanol.

Table 2.1 Analytical data

Compound	Empirical formula	Melting point (°C)	Analytical data Found (Calculated) %		
			C	H	N
HL^1	$C_{19}N_4H_{22}S$	170	67.63	6.70	16.54
			(67.45)	(6.50)	(16.57)
HL^2	$C_{19}N_4H_{16}S$	135	68.25	4.77	16.48
			(68.67)	(4.82)	(16.86)

2.4.2. Crystal structure of HL^1

The molecular structure of HL^1 along with the atomic numbering scheme is given in Fig. 2.2. The compound crystallizes as monoclinic lattice with space group $P2_1/n$ and the molecule shows an Z configuration with respect to the C8 = N3 bond. A torsion angle value of -174.31° corresponding to the S1–C7–N2–N3 moiety confirms the trans configuration of the thiocarbonyl S1 atom with respect to the hydrazine nitrogen atom N3. This is in accordance with the data available for the unprotonated thiosemicarbazones [8].

The C7–S1 bond distance (1.675 Å) is close to that expected for a C=S double bond (1.60 Å) and the C8–N3 bond length (1.290 Å) is nearly the same as that of the C=N double bond length, (1.28 Å). Similarly, the N2–N3 bond length (1.367 Å) is closer to that of single bond length (1.45 Å) than to double bond length (1.25 Å) [9]. These data are in strong support of the existence of 2-benzoylpyridine *N*(4)-cyclohexyl thiosemicarbazone, in the thione form in the solid state. The mean plane deviation calculations show that the pyridyl ring Cg(1) is planar with a max deviation of -0.0096 Å. The thiosemicarbazone moiety also is planar with a maximum mean plane deviation value of -0.0596 Å and a torsion angle value of 3.65° for N2–N3–C8– C9 confirms that the C8–C9 bond is in the same plane as the thiosemicarbazone moiety. Also, the atoms C9, N4, C10, C11, C12, C13 and C8 are coplanar as evidenced from the maximum deviation value of 0.0205 Å from the plane. The dihedral angle formed by the two least square planes Cg(3) and Cg(1) is equal to 67°, which confirms the non-planarity of the two rings. {Cg(1) is the plane consisting of atoms N(4),C(9), C(10), C(11), C(12),C(13) and Cg(3) is the plane consisting of atoms C(14), C(15), C(16), C(17), C(18), C(19) respectively}.

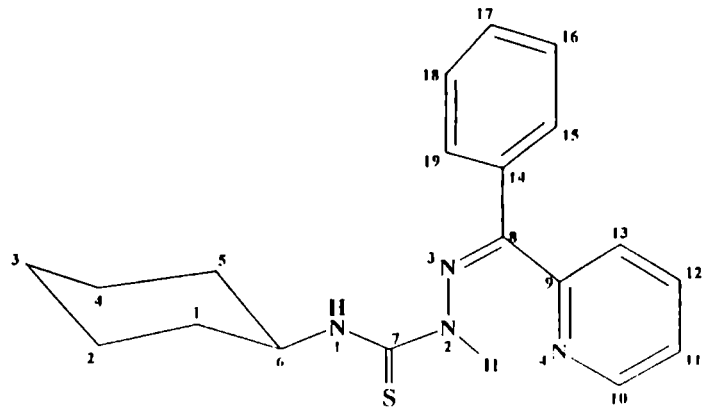

Fig.2.2. Structure of HL[1]

The intramolecular hydrogen bonding interaction N(1) – H(1)N(1)---N(3) leads to the formation of a five membered ring comprising of N(1), H(1)N(1), C(7), N(2) and N(3). A similar six membered ring involving N(2), H(1)N(2), N(3), C(8), C(9) and N(4) is also developed by the N(2) – H(1)N(2) --- N(4) intramolecular hydrogen bonding interaction in the compound. The axial substitution of the cyclohexyl ring at the N1 nitrogen of the thiosemicarbazone is confirmed by a torsion angle value of -178.26° for the N2 – C7 – N1 – C6 bond. Ring Puckering Analysis and least square planes calculations show that the cyclohexyl ring, Cg(2) adopts a chair conformation (Q_T = 0.5701 Å). Atoms C1, C2, C4 and C5 constitute the best fitting plane of the cyclohexyl ring, and atoms C3 and C6 deviate by 1.2462 and 1.2358 Å respectively, on either side of this plane.

The packing of the molecule in a unit cell is shown in Fig. 2.4. The unit cell is viewed down the '*a*' axis and four molecules of the compound are arranged in the unit cell. It is evident from the figure that the unit cell, as a whole, is packed in a centrosymmetric manner. The self-assembly of molecules in the crystal lattice in this manner is effected by the $\pi - \pi$ interaction between the two pyridyl rings, i.e., Cg(1) of the two neighbouring units are observed at a distance of 3.8582 Å

whereas these are observed at an average distance 5.7295Å between the Cg(1) of one unit with the phenyl ring Cg(3) of the adjacent molecule.

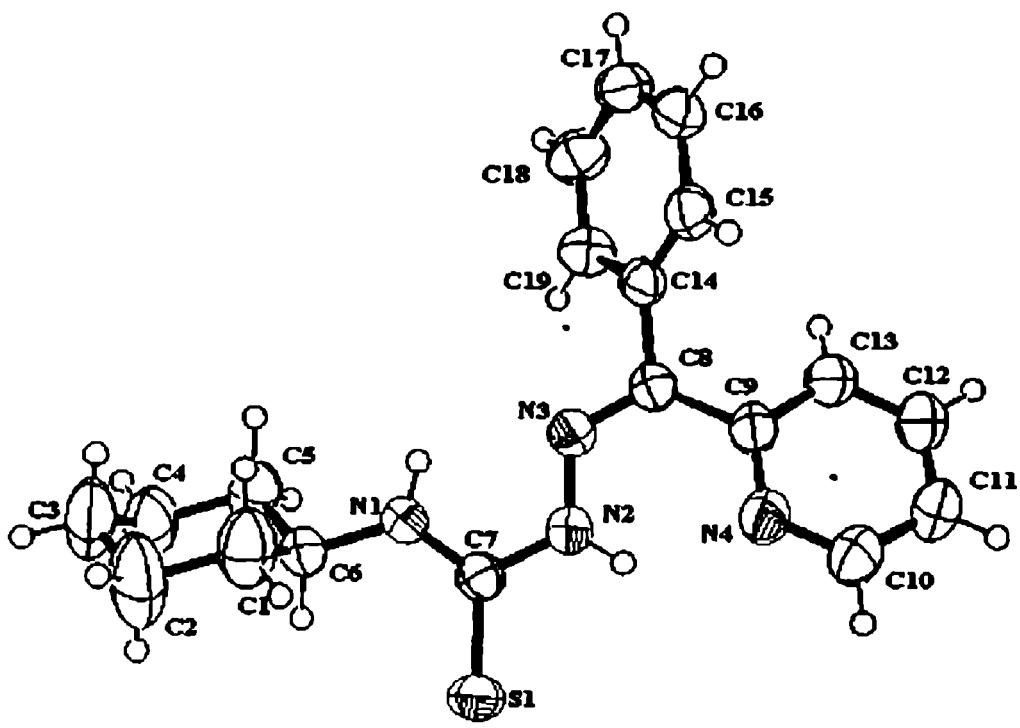

Fig. 2.3. ORTEP diagram for HL^1, displacement ellipsoids are drawn at 50% probability level and hydrogen atoms are shown as small spheres of arbitrary radii.

Table 2.2 Summary of crystal data and structural refinement for HL^1

Empirical Formula	$C_{19}H_{22}N_4S$
Formula weight (M)	338.47
Temperature (T) K	293(2)
Wavelength (Mo K) (Å)	0.71073
Crystal system	Monoclinic
Space group	$P2_1/n$
Lattice constants	
a (Å)	6.1522(3)
b (Å)	17.9701(8)
c (Å)	16.9023(7)
α (°)	90.00
β (°)	94.423(1)
γ (°)	90.00
Volume V (Å^3)	1863.08(15)
Z	4
Calculated density (ρ) (Mg m^{-1})	1.207
Absorption coefficient (μ) (mm^{-1})	0.181
F(000)	720
Crystal size (mm)	0.86x 0.38 x 0.32
θ Range for data collection	2.42- 28.30
Limiting Indices	$-7 \le h \le 8, -19 \le k \le 23, -22 \le l \le 21$
Reflections collected	4559
Unique Reflections	3581 [R_{int} = 0.0169]
Completeness to θ	28.29 (91.1 %)
Max. and min. transmission	0.9444 and 0.8599
Refinement method	Full-matrix least-squares on F^2
Data / restraints / parameters	4559/0/297
Goodness-of-fit on F^2	1.047
Final R indices [$I > 2\sigma(I)$]	R_1 = 0.0452, wR_2 = 0.1228
R indices (all data)	R_1 = 0.0587, wR_2 = 0.1374
Largest difference peak and hole (e Å^{-3})	0.298 and -0.233

Table 2.3 Selected bond lengths (Å) and bond angles (°) of HL^1

C(1) – C(6)	1.499(3)	N(1) – C(6) – C(5)	109.43(14)
C(5) – C(6)	1.525(2)	N(1) – C(6) – C(1)	111.57(15)
C(6) – N(1)	1.452(19)	C(6) – N(1) – C(7)	125.92(13)
C(7) – N(1)	1.328(19)	N(1) – C(7) – S(1)	125.62(11)
C(7) – S(1)	1.675(15)	N(2) – C(7) – S(1)	118.87(11)
C(7) – N(2)	1.364(18)	N(1) – C(7) – N(2)	115.51(13)
N(2) – N(3)	1.367(17)	N(2) – N(3) – C(8)	120.14(12)
C(8) – N(3)	1.290(18)	N(3) – C(8) – C(9)	126.94(13)
C(8) – C(14)	1.489(2)	C(9) – C(8) – C(14)	118.95(12)
C(8) – C(9)	1.488(2)	N(4) – C(9) – C(8)	118.25(13)
C(9) – N(4)	1.345(2)	C(8) – C(9) – C(13)	120.04(14)
C(10) – N(4)	1.337(2)	N(4) – C(9) – C(13)	121.62(14)
C(9) – C(13)	1.391(2)	C(8) – C(14) – C(19)	119.82(13)
C(14) – C(15)	1.393(2)	C(8) – C(14) – C(15)	121.17(14)
C(14) – C(19)	1.384(2)	C(15) – C(14) – C(19)	118.99(14)

Table 2.4. H bonding, π----π and *CH*----π interactions of HL[1]

H bonding (Å, °)				
D-H---A	D-H	H---A	D---A	D- H---A
N1-H1N1---N3	0.87	2.15	2.5905	117
N2-H1N2-N4	0.90	2.01	2.6853	131

H----π interactions			
Cg(I)-Res(I)----Cg(J)	Cg-Cg(Å)	α (°)	β(°)
Cg(1)-[1]----Cg(1)[a]	3.8582	0.00	13.64
Cg(1)-[1]----Cg(3)[b]	5.4642	67.00	53.66
Cg(3)-[1]----Cg(1)[c]	5.9949	69.28	48.82
Eqivalent position codes:	a=-x, 1-y, -z	Cg(1)=N(4),C(9), C(10), C(11),	
	b=-1+x, y, z	C(12),C(13)	
	c= ½ +x, ½-y, ½ +z	Cg(2)=C(1), C(2), C(3), C(4), C(5), C(6)	
		Cg(3)=C(14), C(15), C(16), C(17), C(18),	
		C(19)	

***CH*----π interactions**			
X-H(I)----Cg(J)	H..Cg(Å)	X-H..Cg (°)	X..Cg(Å)
C(3)-H(3B)----Cg(3)[d]	2.8680	139.71	3.6608
Equivalent position code: d = -x, 1-y, 1-z			

D=Donor, A=acceptor, Cg=Centroid. α=dihedral angles between planes I & J, β= angle Cg(I)-Cg(J)

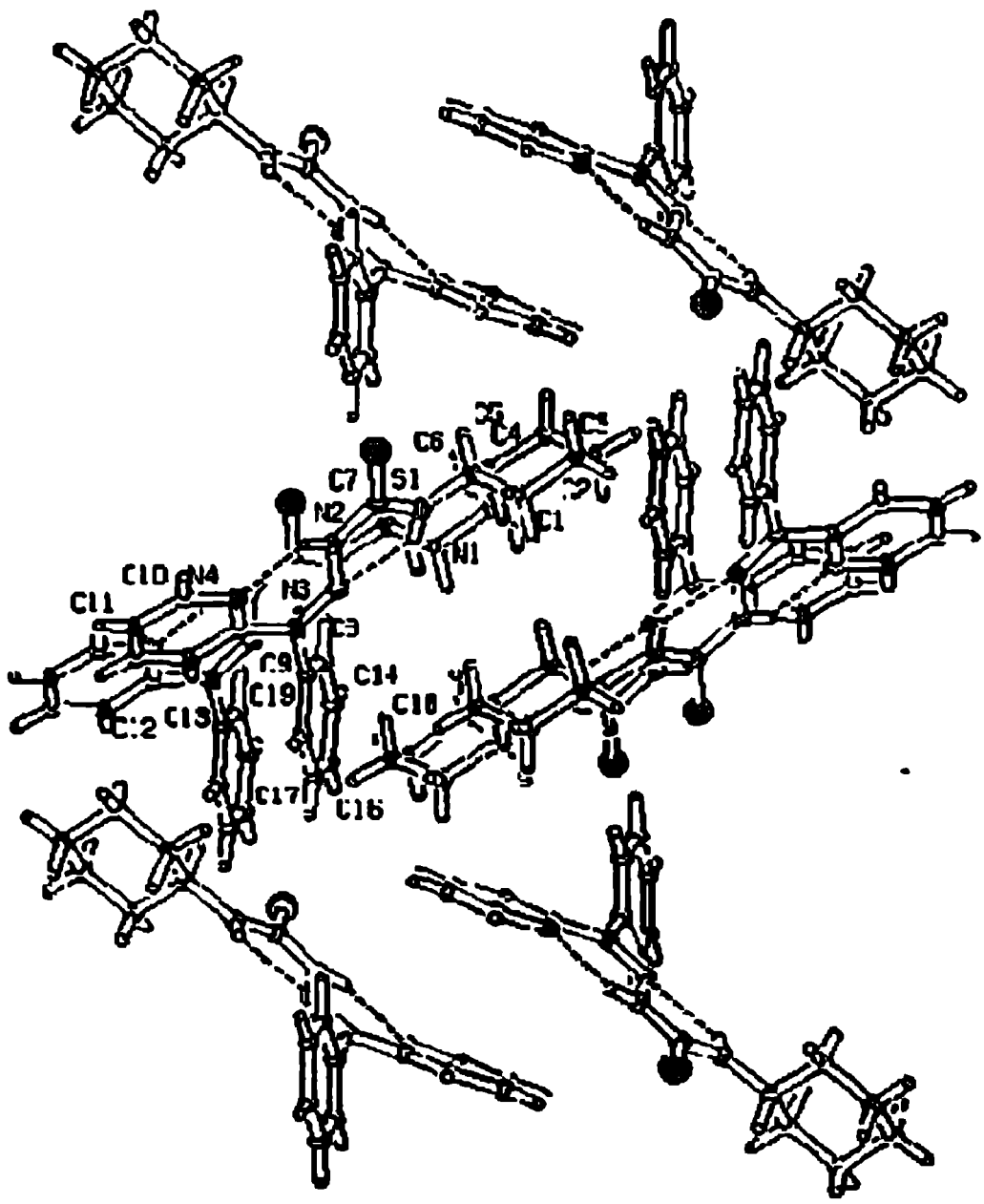

Fig. 2.4. Unit cell packing diagram of HL^1, viewed along the 'a' axis

2.4.3. Infrared spectra

The IR spectral bands are assigned based on the positions of the atoms as shown in Fig. 2.1. The IR spectra of the two ligands HL^1 and HL^2 contain strong broad bands at 3334 and 3423 cm^{-1} due to $\nu(^4NH)$ [10].

The bands at 833 and 835 cm^{-1} in the spectra of ligands HL^1 and HL^2 are due to the $\nu(C=S)$ band. The presence of the $\nu(C=S)$ band and the absence of the $\nu(S-H)$ band, which should be in the range 2600-2550 cm^{-1} suggest that the two ligands remain in the thione form in the solid state [11].

Schiff bases contain C=N stretching band in the range 1471-1689 cm^{-1}. The two thiosemicarbazones HL^1 and HL^2 contain strong bands at 1582 and 1591 cm^{-1} which are due to the $\nu(C=N)$ band. The IR spectral bands of HL^1 and HL^2 observed at 1118 and 1102 cm^{-1} correspond to $\nu(N-N)$ [12,13].

The spectrum of the ligand HL^1 which is 2-benzoylpyridine *N*(4)-cyclohexylthiosemicarbazone contains a strong band at 1447 cm^{-1} which corresponds to cyclohexyl ring [11].

Aromatic and heteroaromatic compounds display strong out-of-plane C-H bending and ring bending absorption bands in the 900-650 cm^{-1} region. The bands at 607 and 622 cm^{-1} in the spectra of HL^1 and HL^2 can be assigned as due to the in-plane ring deformation band of the pyridine ring [14].

2.4.4. Electronic spectra

In the solid-state reflectance spectra of HL^1 and HL^2, the bands observed at *ca.* 341 and 288 nm are assigned to the $n \rightarrow \pi^*$ transitions of the thioamide group and pyridine nitrogen respectively [15]. The bands observed at 259 and 261 nm in the spectra of HL^1 and HL^2 respectively are assigned to the $\pi \rightarrow \pi^*$ transition. In the

spectra from the DMF solution, these bands are blue shifted to 332, 280 and 255 nm having logε values 4.13, 3.38 and 4.20 and respectively.

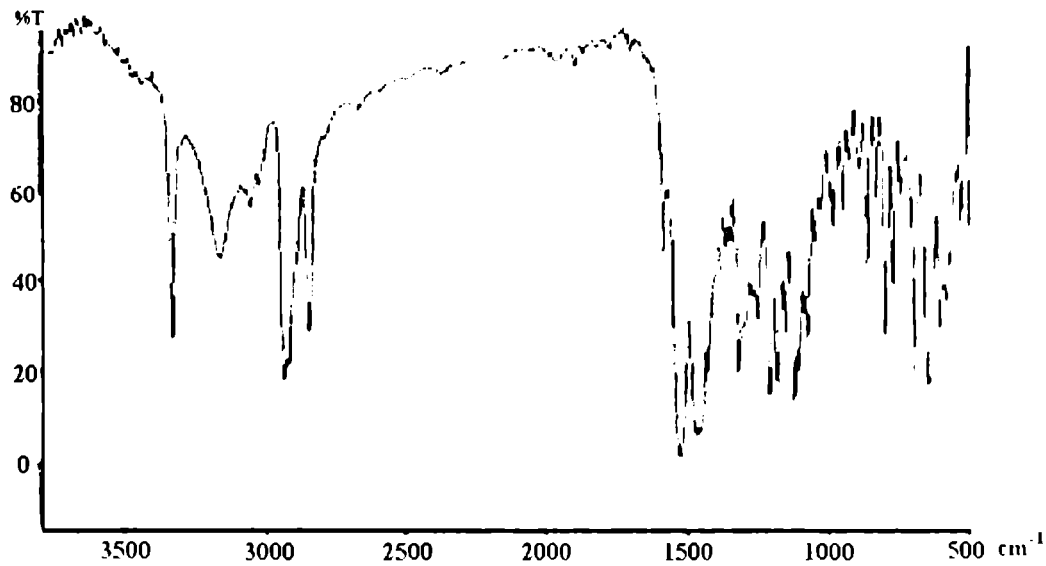

Fig 2.5. IR spectrum of HL^1

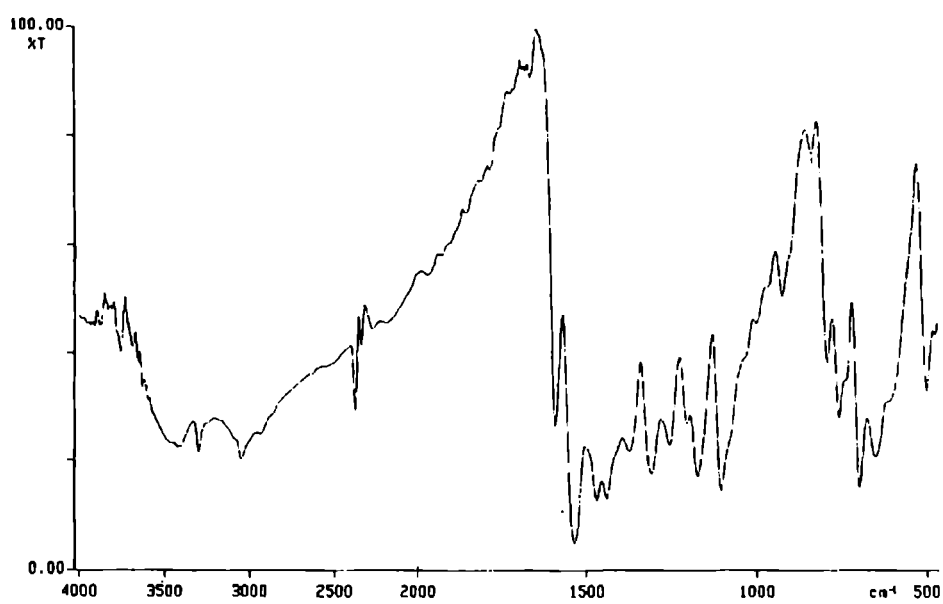

Fig 2.6. IR spectrum of HL^2

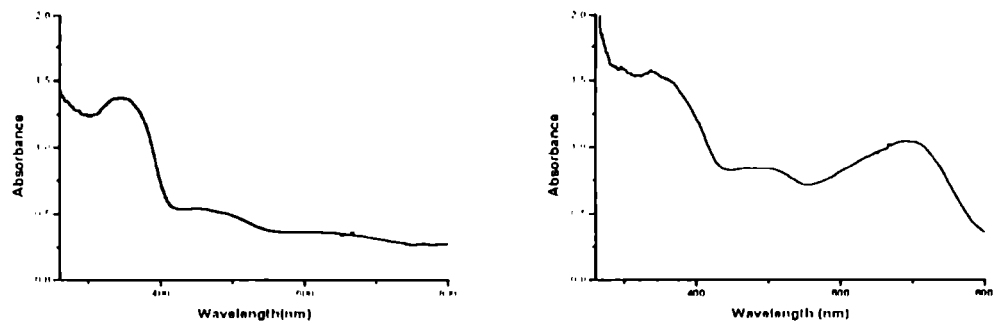

Fig. 2.7. Electronic spectra of HL^1 and HL^2

2.4.5. NMR spectrum of HL^1

^1H NMR spectrum of the ligand HL^1 is recorded in $CDCl_3$. The one-dimensional and two dimensional nuclear magnetic resonance spectra are used in resolving the carbon and hydrogen atoms of HL^1 and the assignments are based on the structure shown in Fig 2.8. The ^1H resonances are assigned on the basis of the chemical shift values, multiplicities and coupling constants and connectivity from ^1H and ^1H-^1H correlation experiments [11,16]. These give insight into the average effective magnetic fields present, interaction of the nuclear spin with the adjacent atoms and the number of equivalent protons.

The NMR spectral assignments are based on the positions of the atoms given in Fig. 2.8, which is based on the X-ray diffraction studies of HL^1 which has been already mentioned in section 2.4.2. The ^1H NMR spectrum reveals four signals for the pyridyl moiety, multiplet for the phenyl moiety and seven well-resolved peaks for the cyclohexyl moiety. The signals at δ =13.48 and 7.63 ppm are assigned to the ^2NH and ^1NH protons respectively [17]. The intensity of these peaks decreases on the addition of D_2O, which suggests that they are easily exchangeable. These protons are shifted downfield because they are attached to

heteroatoms and so are easily subjected to hydrogen bonding and are decoupled by the electrical quadrupole effects. The proton attached to ^{2}N appears as singlet as expected since the NH protons are decoupled from the nitrogen atoms and the protons from the adjacent atoms. But contrary to this, ^{1}NH shows coupling with the adjacent hydrogen H6 and hence gives a doublet. This coupling is clear in COSY (correlation spectroscopy), which can be attributed to the low NH exchange rate. The peak at 8.80 ppm is due to the H10 proton.

This proton is very sensitive to the electron densities as it is close to the pyridyl nitrogen and is observed to be deshielded due to the electronic effect of the phenyl ring. The phenyl moiety appears as a multiplet at about 7.45 ppm where the chemical shift values are very close and hence it is very difficult to be resolved. The complexity of the COSY predicts that the spectrum is not strictly of the first order. The peaks (7.3 ppm) corresponding to the solvent ($CDCl_3$) appear to be superimposed with that of the phenyl protons. The cyclohexyl moiety forms a chair conformation and hence puts the hydrogen in two different electronic environments, *viz*, axial and equatorial and hence gives seven well-resolved peaks. The equatorial protons (H5e - 2.08 ppm) are found to resonate at a slightly higher frequency than that of the axial protons (H5a - 1.27 ppm). A multiplet present at 4.32 ppm is attributed to the H6, which is deshielded by the adjacent electronegative nitrogen.

Fig. 2.10. shows the ^{1}H-^{1}H-correlation spectral assignments of the compound. The COSY separates out the interactions among the protons and establishes the proton-proton couplings. The proton spectrum is plotted along the X and Y-axes and can be seen as contours in diagonal. In the proton NMR spectrum we have already identified a doublet at 8.80 ppm as of pyridyl proton H10.

In the proton NMR spectrum we have already identified a doublet at 8.80 ppm as of pyridyl proton H10.

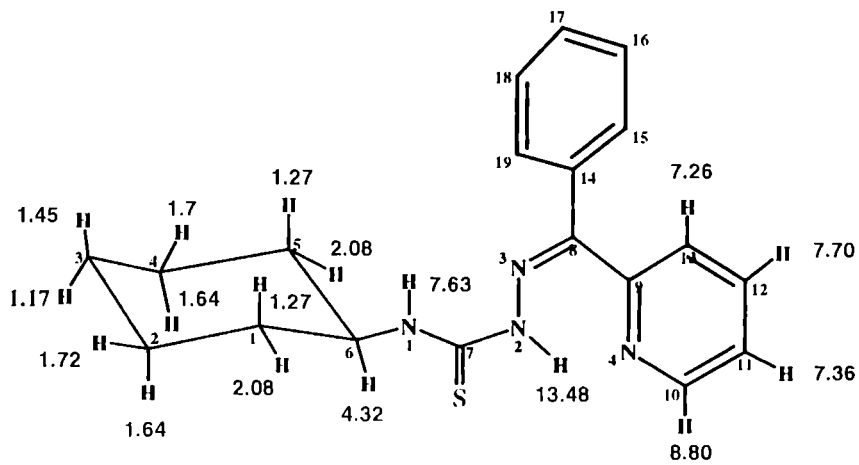

Fig 2.8. ^{1}H NMR spectral assignments of HL^1

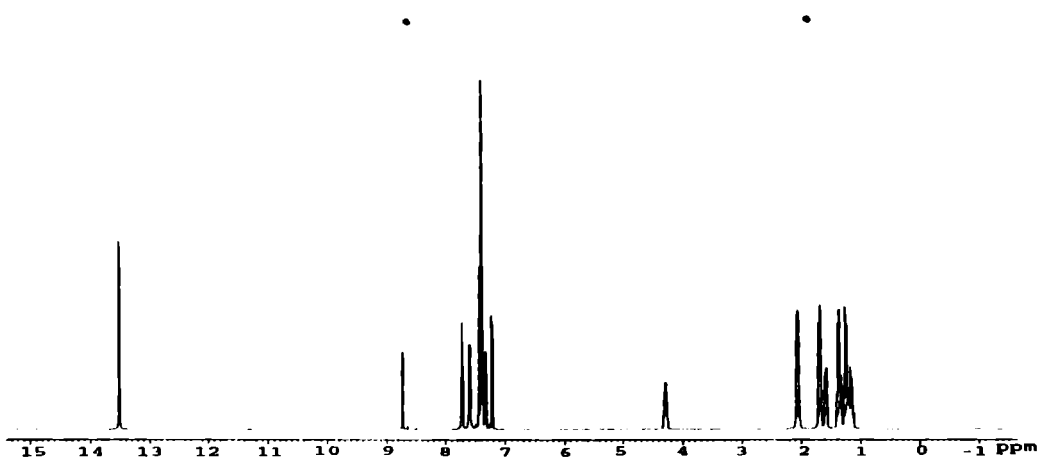

Fig. 2.9. ^{1}H NMR spectrum of HL^1

off diagonal spots at 8.86 ppm (H10) and 7.70 ppm (H12). The multiplet at 7.36 ppm is related to the number of possible orientations these neighboring protons can adopt. The H12 proton is also split by H13 proton and vice versa. In the spectrum around δ = 7.40 ppm, the contours are seen ambiguous and the multiplet is assigned to the protons of the phenyl moiety. The chemical shifts are very close, so this spectrum is not strictly first order. The peak at 2.08 ppm is assigned to the equatorial proton on the carbon atom C5. From the COSY, it is shown to interact with three other protons H6, H5a and H4e. The couplings are of diequatorial and axial/equatorial type. The coupling constants agree well with those corresponding to the chair conformation of cyclohexane. Similarly the H5e and H4e protons split the peak of the axial proton H5a. In the ^{1}H NMR the multiplet at 1.72 ppm is assigned to the H4e proton, which interacts with five other protons H5a, H5e, H4a, H3e and H3a, where interaction with H3a is very weak. All these couplings are of vicinal type.

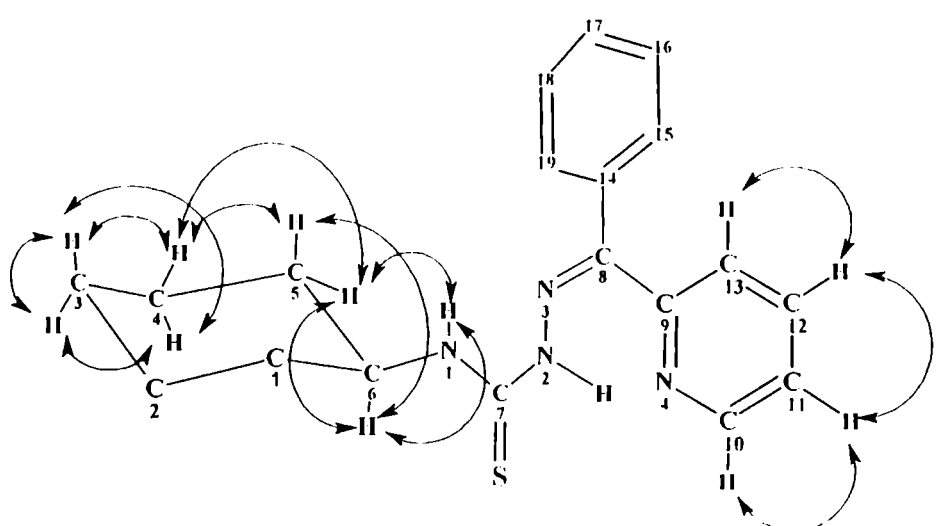

Fig. 2.10. ^{1}H - ^{1}H COSY assignments of HL^1

The coupling of the H4a proton with the neighboring H4e, H3a and H3e protons forms the multiplet at 1.64 ppm. This proton shows no coupling with the

H5e and H5a protons. The coupling between the H3a and H4a protons gives J value around 11 Hz, which is consistent with diaxial type coupling constants. Even though the coupling in the region 1.5 ppm is difficult to resolve, as the chemical shift values of H3a, H3e and H5a are very close, it is clearly evident from the spectrum that the H3a proton couples with the H4a and H3e protons. Similarly the H3e is coupled with H3a, H4e and H4a protons. The same coupling is observed for the protons at C1 and C2, which are magnetically equivalent to the C5 and C4 protons. The H6 proton interacts with the ^{1}NH and also with two protons of C1 and C5.

The ^{13}C NMR spectrum was assigned on the basis of the proton-decoupled ^{13}C spectrum and the HMQC (heteronuclear multiple quantum coherence). The HMQC experiment provides the correlation between the protons and their attached heteronuclei through the heteronuclear scalar coupling. The decoupled ^{13}C spectrum of the compound contains 15 peaks corresponding to fifteen magnetically unique atoms. The signal from the ^{13}C spectrum is much weaker than that of the corresponding proton NMR. From the HMQC, it is evident that the peaks at 177.02, 152.52 and 148.72 ppm are of the non-protonated carbons and they correspond to the S=C7, N=C8 and C9 carbon atoms respectively. The carbon atom closest to the electronegative atom is farthest downfield. The carbon atoms on the pyridyl ring can be assigned as C10 142.38, C11 137.81, C12 124.11, C13 126.05. Aromatic carbons of the phenyl ring appear around 129 ppm and it is very difficult to be resolved. The peaks at 32.74, 24.89, 25.61 and 52.85 ppm are assigned to the C1, C2, C3 and C6 carbons respectively. The C4 and C5 are chemically equivalent with the C2 and C1 carbons and hence have the values 24.89 and 32.74 ppm respectively.

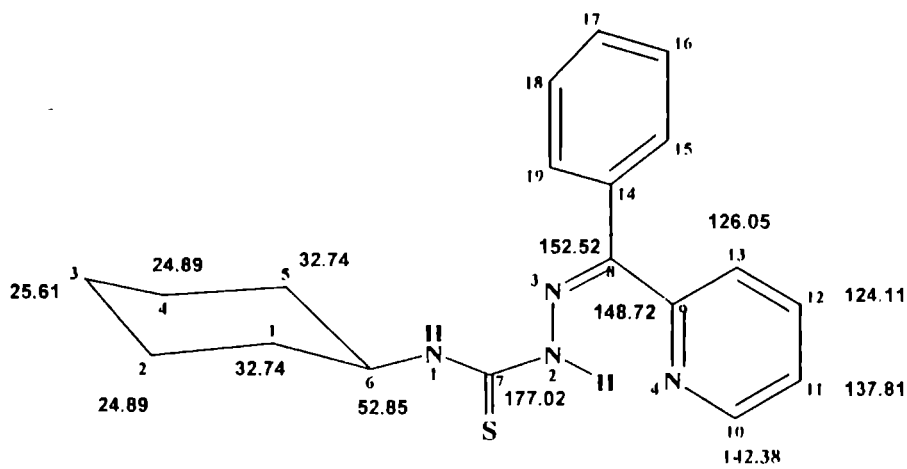

Fig. 2.11. ^{13}C NMR spectral assignments of HL^1

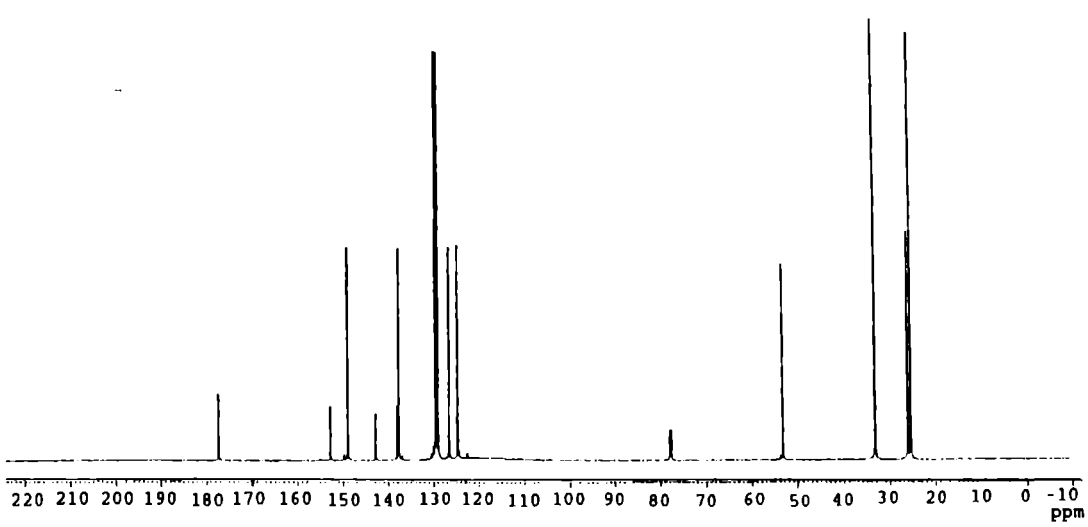

Fig. 2.12. ^{13}C NMR spectrum of HL^1

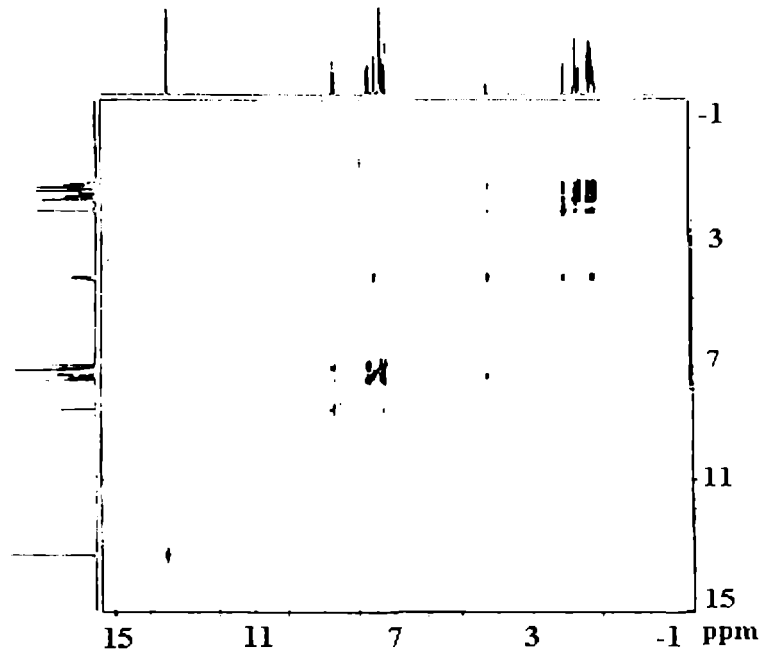

Fig. 2.13. ^{1}H-^{1}H COSY spectrum of HL^{1}

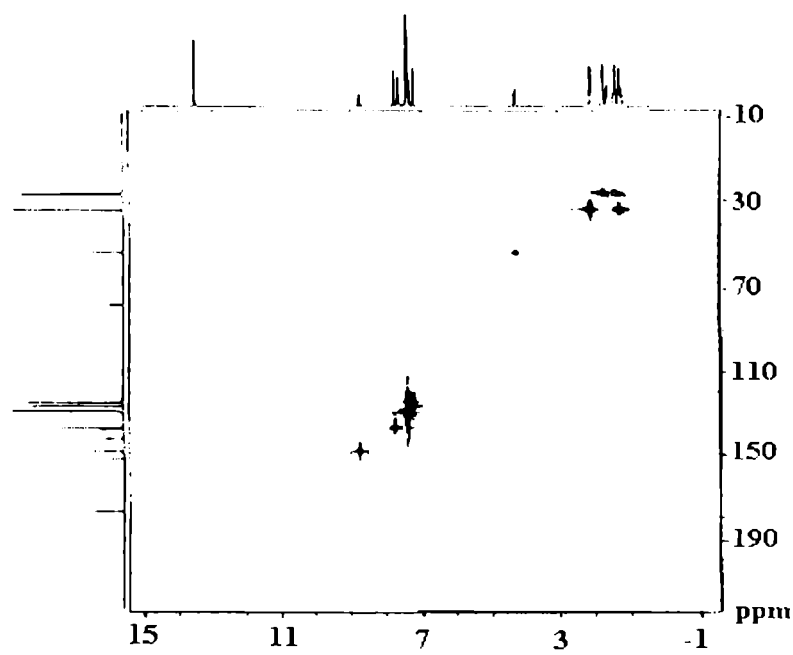

Fig. 2.14. ^{13}C-^{1}H HMQC spectrum of HL^{1}

2.4.6. NMR spectrum of HL^2

^1H and C^{13} NMR spectra of the compound were recorded in $CDCl_3$ and the assignments are based on earlier works [17,18]. ^1H NMR. spectrum of HL^2 shows signals at δ = 14.06 (s,1H), 8.83 (d,1H) and 9.53 (s,1H) which correspond to the ^2N-H, C(10)-H, and ^1N-H respectively. The downfield value of ^1N-H proton is due to the deshielding effect of the phenyl group. The aromatic protons of the two phenyl groups and the three protons of the pyridine ring appear at δ values in the range 7.2 -7.8. The signals are at δ= 7.79 (m, 1H), 7.69 (d, 2H), 7.56 (m, 2H), 7.48 (m, 3H), 7.38 (m, 4H), 7.22 (m, 1H). The absence of peaks corresponding to the S-H proton in the spectrum supports the fact that in solution, the predominant tautomer is in the thione form.

The ^{13}C NMR spectrum was assigned on the basis of the proton-decoupled ^{13}C spectrum. The decoupled ^{13}C spectrum of the compound contains 15 peaks corresponding to the fifteen magnetically unique atoms. Pair of carbon atoms C1-C5, C2-C4, C15-C19, C16-C18 are magnetically equivalent. In the ^{13}C NMR spectrum of HL^2, the signals observed were assigned values based on earlier works. The peaks at 176.65, 152.45 and 148.72 ppm correspond to S=C7, N=C8 and C9 carbon atoms. The carbon atoms on the pyridyl ring can be assigned as C10 142.79, C11 136.59, C12 124.18, and C13 126.45. Aromatic carbons of the two phenyl rings appear around 129 ppm and it is very difficult to be resolved.

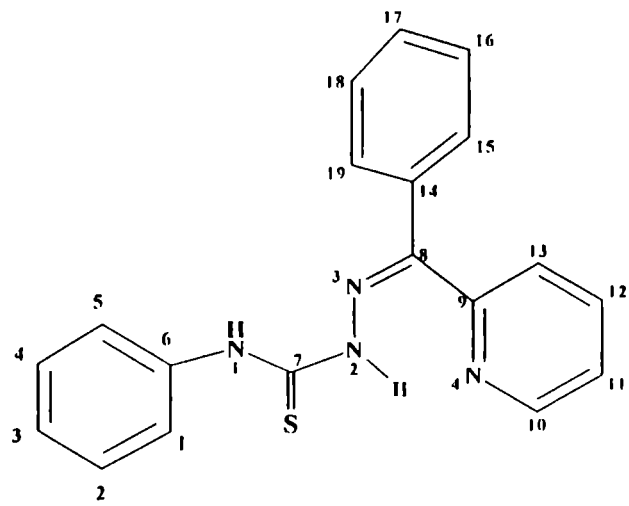

Fig.2.15. Structure of HL^2

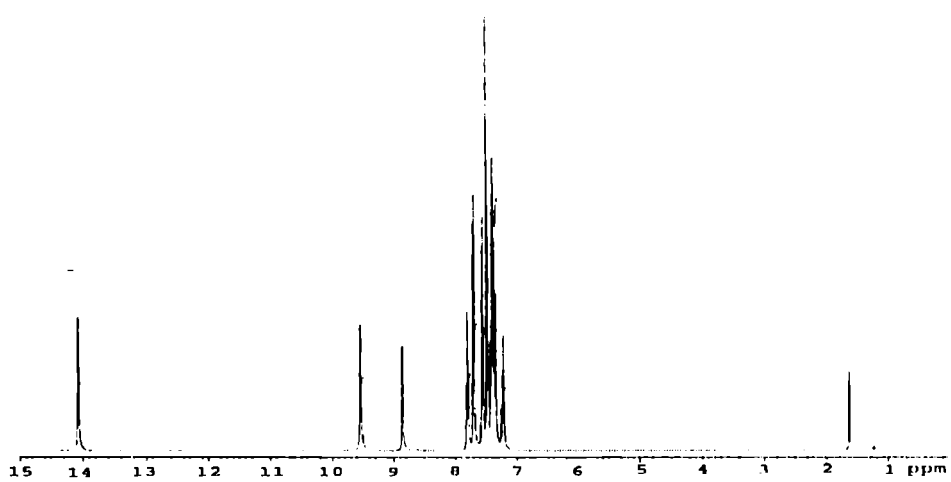

2.16. ^1H NMR spectrum of HL^2

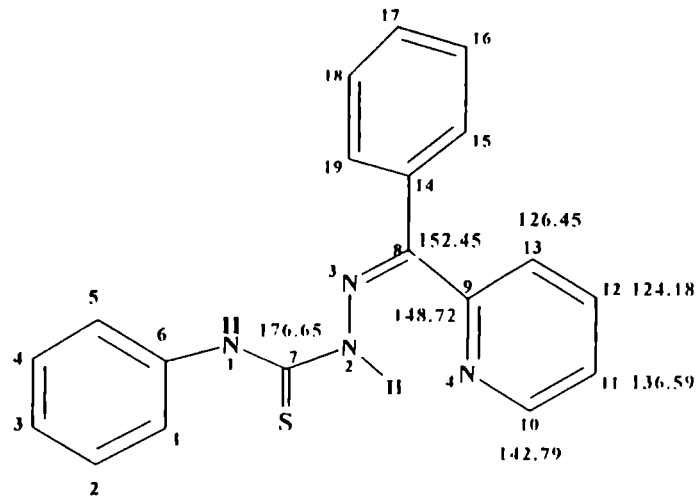

Fig.2.17. ^{13}C NMR spectral assignments of HL^2

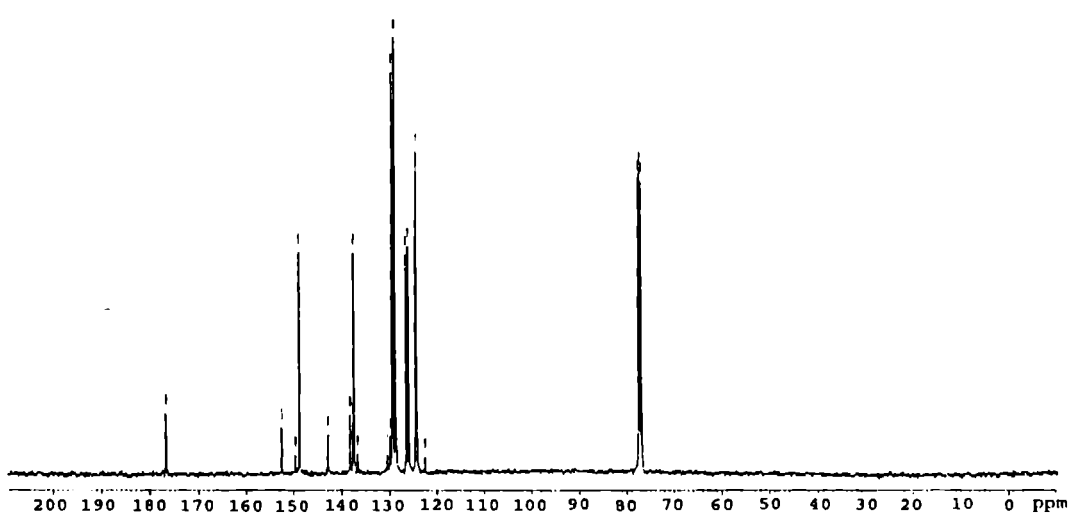

2.18. ^{13}C NMR spectrum of HL^2

References

1. D.L. Klayman, J.F. Bartosevich, T.S. Griffin, C.J. Mason, J.P. Scovill, J. Med. Chem. 22 (1979) 855.
2. P. Bindu, M.R.P. Kurup, T.R. Satyakeerty, Polyhedron 18 (1999) 321.
3. R.P. John, A. Sreekanth, M.R.P. Kurup, S.M. Mobin, Polyhedron 21 (2002) 2515.
4. M.R.P. Kurup, M. Joseph, Synth. React. Inorg. Met-Org Chem. 33 (2003) 1275.
5. D.X. West, G.A. Bain, R.J. Butcher, J.P. Jainski, Y. Li, R.Y. Pozdniakiv, J. Vades-Martinez, R.A. Toscano, S. Hernandes-Ortega, Polyhedron 15 (1996) 665.
6. A. Usman, I.A. Razak, S. Chantrapromma, H.K. Fun, V. Philip, A. Sreekanth, M.R.P. Kurup, Acta Crystallogr. C 58 (2002) 652.
7. M.B. Ferrari, G. Fava, C. Pelizzi, P. Tarasani, J. Chem.Soc., Dalton Trans. (1992) 2153.
8. D. Chattopadhyay, T. Banerjee, S.K. Mazumdar, S. Ghosh, R. Kuroda, Acta Crystallogr., Sect.C. 43 (1987) 974.
9. J.March, Advanced Organic Chemistry, Reactions, Mechanisms and structure, 4th ed.,Wiley, New York, 1992.
10. D.X. West, N.M. Kozub, G.A. Bain, Transition Met. Chem. 21(1996) 52.
11. R.M. Silverstein, G.C. Bassler, T.C. Morrill, Spectrometric Identification of Organic Compounds, 4th ed., Wiley, New York, 1981.
12. D.X. West, A.M. Stark, G.A. Bain, A.E. Liberta, Transition Met. Chem. 21 (1996) 289.
13. H. Beraldo, A.M. Barreto, R.P. Vieira, A.P. Rebolledo, N.L. Speziali, C.B. Pinheiro, G. Chapuis, J.Mol. Struct. 645 (2003) 213.

14. D.X. West, I.S. Billeh, J.P. Jesinski, J.M. Jesinski, R.J. Butcher, Transition Met. Chem. 23 (1998) 209.

15. V.Philip, V.Suni, M.R.P. Kurup, M.Nethaji, Polyhedron 23 (2004) 1225.

16. W.Kemp, Organic spectroscopy, 3rd ed., Macmillan Press Ltd.,Hampshire, 1996.

17. D.X. West, H. Gebremedhin, T.J. Romack, Transition Met. Chem.19 (1994) 426.

18. D.X. West, J.S. Ives, J. Krejct, M.M. Salberg, T.L. Zumbahlen, G.A. Bain, A.E. Liberta, Polyhedron 14 (1995) 2189.